A THESIS FOR THE DEGREE OF MASTER OF SCIENCE

# Analyzing the relationship between photothermal ratio and fruit yield through simulating an explanatory crop model that reflects fruit-setting pattern of sweet peppers

# 착색 단고추의 착과 패턴을 반영한 설명적 모델의 시뮬레이션을 통한 광열 비율과 수확량의 관계 분석


BY

HAMIN YOON



AUGUST, 2023

MAJOR IN HORTICULTURAL SCIENCE AND BIOTECHNOLOGY

DEPARTMENT OF AGRICULTURE, FORESTRY, AND BIORESOURCES

THE GRADUATE SCHOOL OF SEOUL NATIONAL UNIVERSITY

# Analyzing the relationship between photothermal ratio and fruit yield through simulating an explanatory crop model that reflects fruit-setting pattern of sweet peppers

**UNDER THE DIRECTION OF DR. TAE IN AHN**
**SUBMITTED TO THE FACULTY OF THE GRADUATE SCHOOL OF**
**SEOUL NATIONAL UNIVERSITY**

**BY**
**HAMIN YOON**

**MAJOR IN HORTICULTURAL SCIENCE AND BIOTECHNOLOGY**
**DEPARTMENT OF AGRICULTURE, FORESTRY, AND BIORESOURCES**

**AUGUST, 2023**

**APPROVED AS A QUALIFIED DISSERTATION OF HAMIN YOON**
**FOR THE DEGREE OF MASTER OF SCIENCE**
**BY THE COMMITTEE MEMBERS**

CHAIRMAN

Hyo Beom Lee, Ph.D.

VICE-CHAIRMAN

Tae In Ahn, Ph.D.

MEMBER

Changhoo Chun, Ph.D.

# Analyzing the relationship between photothermal ratio and fruit yield through simulating an explanatory crop model that reflects fruit-setting pattern of sweet peppers

HAMIN YOON

Department of Agriculture, Forestry, and Bioresources

The Graduate School of Seoul National University

## ABSTRACT

Radiation and temperature are essential factors that determine plant photosynthesis and development. Photothermal ratio (PTR), a ratio between daily light integral and daily mean temperature, is an explanatory indicator actively applied in commercial greenhouses for climate control. Although it was reported to have strong linearity with the yield of staple food crops, this relationship might not hold for indeterminate fruit crops whose fruit-setting pattern is affected by the source-sink ratio (SSR). This might complicate the application of PTR in greenhouse climate management. The objective of this study is to analyze the relationship between PTR and fruit yield by simulating an explanatory crop model, INTKAM, and to modify the PTR calculation for a better explanation of sweet pepper growth characteristics. The relationship between the fruit yield of sweet peppers (*Capsicum annuum* L. var. *annuum*) cultivated for three periods and the average PTR during fruit development was

analyzed. The model was calibrated for the winter period 2020 and simulated in 100 randomized radiation-temperature conditions. As a result, the strong linear relationship between fruit yield and PTR was not observed, which was also identified through the simulation study. The weak linearity was attributable to the SSR that regulates flowering depending on its threshold (1.03), which was confirmed with the increased linearity through the simulation without this effect. When the fruit load was taken into account in the PTR calculation ($PTR_{fruit}$), it showed a higher similarity with the SSR change throughout the growth period. Moreover, it was confirmed that the fruit yield was within the specific range of modified PTR (0.5-2.0 mol $m^{-2}$ (fruit + °C)$^{-1}$). These results imply that a crop growth model can be used to interpret the relationship between PTR and fruit yield, considering the internal biological process. In conclusion, $PTR_{fruit}$ is a more useful indicator for greenhouse climate management than PTR.

**Keywords**: explanatory model, indeterminate fruit crop, photothermal ratio, source-sink ratio

**Student number**: 2021-25491

# CONTENTS

# LIST OF TABLES

# LIST OF FIGURES

# INTRODUCTION

Radiation and temperature have a combined effect on the photo-assimilate balance because radiation affects the amount of carbohydrates that plants assimilate, while temperature affects the consumption of carbohydrates through respiration and plant development. Therefore, when radiation levels outweigh temperature, plants may excessively assimilate without corresponding growth. Conversely, if radiation is not sufficient to supply photo-assimilates while the temperature is high, it can hinder the translocation of photo-assimilates to other plant organs, resulting in a limited growth rate (Li et al., 2015). Both situations are detrimental to the long-term cultivation of fruit crops. Therefore, the photo-assimilate balance should be stabilized by adjusting the temperature according to the daily radiation level or vice versa (Elings et al., 2006).

In commercial greenhouses, growers and consultants control radiation and temperature levels based on climate management variables such as the photothermal ratio (PTR), which is defined as the ratio between the daily light integral (DLI) and the daily mean temperature (DMT) (Geelen et al., 2021; Liu and Heins, 1997). In order to transform the empirical usage of PTR in greenhouses into a scientific concept, several scientists have attempted to quantify plant growth traits or predict the developmental stage of plants using PTR or other photothermal metrics (Elings et al., 2006; Xu et al., 2010). For example, PTR has a strong linear relationship with wheat

yield or flower development because they are directly affected by photoperiod, radiation level, and temperature (Menéndez and Satorre, 2011; Liu and Heins, 2002).

It has been suggested that crops such as sweet peppers form fruits when the balance between the assimilation and consumption of photo-assimilates, known as the source-sink ratio (SSR), is higher than the specific threshold (Heuvelink et al., 2004; Wubs et al., 2009). SSR is defined as the ratio between source strength and sink strength, which is affected by radiation and temperature (Li et al., 2015). That is, the reported linear relationship between the PTR and yield might not apply to indeterminate fruit crops due to the complexities of how their current state affects the subsequent performance of plant growth (Elings and de Visser, 2011). However, less attention has been paid to this relationship, although climate control significantly regulates fruit yield. Hence, a theoretical discussion is needed for the technical application of PTR in a commercial greenhouse.

To mechanistically understand this intricate process, an explanatory model can be utilized. It describes the internal process of plant growth using mathematical formulas. Thus, it can help identify the complex relationship between the environment and plant growth characteristics.

The objective of this study is to investigate the relationship between PTR and the yield of indeterminate fruit crops. On top of that, the study aims to modify the way PTR is calculated to improve its representativeness as a plant balance indicator. It is hypothesized that their relationship might be affected by the irregular fruit setting pattern of sweet peppers, which is controlled by SSR. An explanatory crop model,

INTKAM, was used to estimate fruit yield and understand the underlying mechanism in this relationship. This approach is expected to help connect PTR variations to internal plant dynamics from a systematical point of view. Additionally, it will narrow the information gap on the PTR as a greenhouse climate management indicator.

# LITERATURE REVIEW

## Explanatory model

Explanatory models aim to describe underlying biophysical principles in plants using mathematical equations and computer programs (Jones et al., 2017). Unlike black-box models, which do not require an understanding of the exact process behind them, explanatory models help scientists understand the effects of components in agricultural systems and their complex interactions (Dingkuhn et al., 2020). This enables scientific explanations as to why specific phenomena occur. Thus, it effectively simulates various scenarios, which helps in agricultural management and policy decision-making.

INTKAM is one of the explanatory models originally developed for cucumbers (Marcelis, 1994). This was further modified to reflect species-specific traits of sweet peppers, eggplants, and tomatoes (Marcelis et al., 2006; Elings et al., 2007; Elings and Visser, 2011). The model explains that the yield of indeterminate fruit crops fluctuates due to the imbalance in photo-assimilate supply and demand. Therefore, the model describes how flowers appear and abort as a function of photo-assimilate balance, which is affected by radiation, temperature, and the number of fruits (fruit load). The model was later adapted to reflect the impact of sink strength on fruit abortion, which explained its stochastic characteristic based on plant growth state (Wubs et al., 2006; Wubs et al., 2012b). After reflecting on this concept, the model improved its accuracy in predicting the fruit set pattern of sweet peppers.

**Photothermal ratio**

The photothermal ratio (PTR), also known as the photothermal quotient, is defined as the ratio of daily light integral (DLI) to daily mean temperature (DMT). PTR plays a crucial role in explaining plant growth and development. PTR can explain the combined effect of DLI and DMT on plants, which impacts various physiological processes such as cell expansion (Johansson et al., 2014), cell division (Van Ittersum et al., 2003), and biochemical reactions (Moore et al., 2021). These processes are fundamental to photosynthesis, respiration, photo-assimilate translocation, and the overall plant development rate.

Initially introduced as the ratio of radiant to thermal energy, the PTR showed a positive correlation with flower quality traits like stem width or fetal area (Liu and Heins, 1997; Liu and Heins, 2002). This approach effectively explains the anthesis of floral crops because it is influenced by both photoperiod and DMT (Moccaldi and Runkle, 2007). Subsequent studies have further established its linear relationship with crop yields, such as the number of seeds in wheat (Menendez and Satorre, 2011), suggesting that it is a consequence of accumulated radiation and temperature. Such studies used the PTR to explain the effect of thermal stress on plants in their sensitive stage, where the number of seeds is determined (Sadras and Dreccer, 2015; Poggio et al., 2005). This concept has been applied to indeterminate fruit crops, where it helps explain the photo-assimilate balance state and assists farmers in setting optimal temperatures based on radiation levels (Elings et al., 2006; Geelen et al., 2021).

Nevertheless, the impact of PTR on fruit yield remains unclear, which complicates the strategic implementation of PTR for maximizing fruit yield.

**Concept of source-sink ratio**

The source is an organ that assimilates carbohydrates through photosynthesis, while the sink is an organ that attracts carbohydrates for their growth and conservation. Accordingly, the rate of such assimilation is defined as source strength, and the rate of such attraction is defined as sink strength (Marcelis, 1996). The ratio of source strength to sink strength is called the source-sink ratio (SSR), representing photo-assimilate balance status (Heuvelink et al., 2004).

Source strength is calculated as the photosynthetic rate subtracted by the maintenance respiration rate. Thus, it is affected by leaf area, radiation, temperature, and carbon dioxide concentration (Sánchez-Molina et al., 2015; Shin et al., 2022).

In contrast, sink strength is quantified by temperature experiments and destructive harvests. Subsequently, it is calculated as the potential growth rate of fruits and vegetative organs in a mild condition (Wubs et al., 2012b). As the plant development rate is mainly driven by temperature, vegetative sink strength is expressed as a linear function of DMT (Li et al., 2015). Thus, when the indoor temperature is relatively consistent, vegetative sink strength is set as a constant value (Kleijbeuker and Lee, 2019).

On the other hand, reproductive sink strength is estimated based on growing degree days (GDD) because the fruit development rate is higher in warmer conditions

(Bertin, 2005). Potential fruit fresh weight is estimated using Richard's function, and this is converted to potential fruit dry weight, which is fruit sink strength, using an empirical function of fruit dry matter content (Wubs et al., 2012a). When calculating reproductive sink strength, the sink strength of each fruit is summed up to reflect the effect of fruit load.

SSR is hypothesized to determine the flower abortion rate of sweet peppers (Wubs et al., 2009). As existing fruits in a plant compete for a limited amount of photo-assimilates, newly formed flowers abort in their critical periods when the fruit load is high or the assimilation rate is low. This is explained as the threshold concept, where flowers only appear and set fruit when the average SSR during their development is higher than a specific threshold. This causes the irregular fruit-setting pattern of indeterminate fruit crops. That is, SSR not only represents the current photo-assimilate state of plants but is also a key variable that regulates the fruit setting pattern of indeterminate crops.

# MATERIALS AND METHODS

## Plant materials, growth conditions, and data collection

Sweet peppers (*Capsicum annuum* L. var. *annuum*) were cultivated three times in a Venlo-type greenhouse located at the experimental farm of Seoul National University in Suwon, Korea (37.3°N, 127.0°E) (Table 1). After a nursery period of six weeks in a commercial greenhouse in Asan, Republic of Korea (36.8°N, 127.1°E), the seedlings were transplanted in rockwool slabs (Grodan GT Master, Grodan, Roermond, The Netherlands). Sweet peppers were pruned to maintain two main stems with trellis strings. PBG nutrient solution was applied, and the EC and pH were maintained at 2.6-3.0 dS $m^{-1}$ and 5.5-6.5, respectively. 133 mL of the nutrient solution was irrigated through drippers whenever the cumulative solar radiation reached 50 J $cm^{-2}$. Temperature data and relative humidity data were collected using a complex sensor (AQ3020, Aosong Electronics, Guangzhou, China), and radiation data was collected using a pyranometer (SP-110, Apogee Instrument Inc., Logan, UT, USA) (Fig. 1 and Table 1). 2.1 μmol $m^{-2}$ $d^{-1}$ $W^{-1}$ was applied as a conversion factor to change the radiation unit from Watt to photosynthetic photon flux density.

Three plants were randomly harvested monthly to investigate the leaf area and total dry weight of the vegetative organs (leaf, petiole, and stem). The leaf area was measured with a leaf area meter (LI-3000 A, LI-COR). The dry weight of organs was measured after drying for 72 h at 105°C in a forced-air drying oven (HB-503LF, Hanbaek CO. LTD, Bucheon-si, Gyeonggi-do, Korea). Twelve plants were randomly

sampled, and their fruits were harvested weekly whenever they were riped. Individual fruit fresh weight was measured with a weighing scale 24 h after harvesting.

Table 1. Information on the three cultivation periods. S and W in the period name are the abbreviations of summer and winter, respectively.

| Period | 2020W | 2021S | 2021W |
|---|---|---|---|
| Usage | Calibration & Yield analysis | Yield analysis | Yield analysis |
| Planting density (Den) (plant $m^{-2}$) | 3.06 | 5.95 | 3.06 |
| Number of plants | 84 | 65 | 36 |
| Cultivar | Mavera & Florate | Mavera & Florate | Mavera |
| Planting date | Aug 26 | Mar 08 | Aug 23 |
| End of Period | Jan 25 | Jul 05 | Jan 19 |

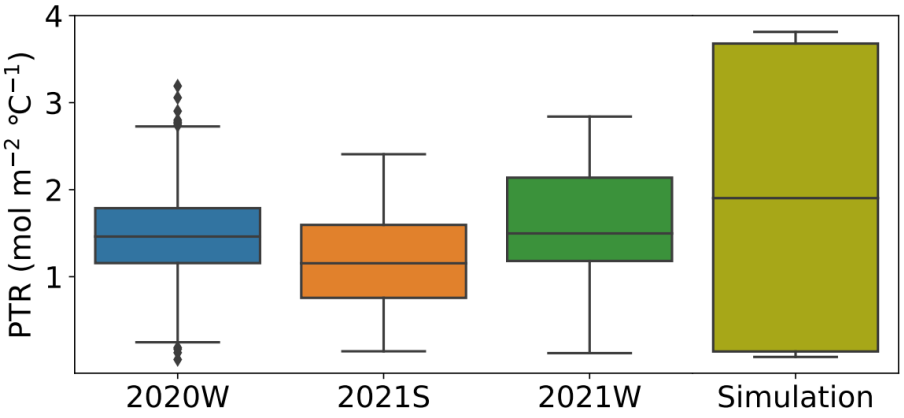


Fig. 1. Distribution of photothermal ratio (PTR) over the three growth periods and 100 simulation datasets.

**Model description**

An explanatory crop model, INTKAM, was used for the simulation, which was modified by Wubs (2021b) in the previous study to reflect the fruit-setting pattern of sweet peppers by considering the effect of source-sink ratio (SSR) on flower and fruit abortion. The model was chosen to investigate the effect of PTR on fruit yield and SSR as it describes the assimilation and consumption of photo-assimilates according to source strength and sink strength, which are expressed as a function of radiation and temperature. Definitions of the parameters and variables that were used can be found in (Table 1-4), and the schematic diagram of the model is illustrated in (Fig. 2). The present study modified some equations to reflect the complexity of how the current state affects the subsequent process of plant growth (Eq. 1 and 16).

Leaf area index (LAI) was estimated by multiplying constant specific leaf area (SLA) and dry matter of leaves on the previous day ($DM_{leaf}(t-1)$) so that leaf area increases based on plant growth state (Eq. 1). LAI was assumed to be constant after the topping of the main stems. The canopy photosynthetic rate was calculated per second using the Farquhar, von Caemmerer, and Berry (FvCB) model and the Lambert-Beer law (Eq. 2-8) (Sánchez-Molina et al., 2015; Shin et al., 2022; Hirose, 2005) as follows:

$$LAI = DM_{leaf}(t-1) \cdot SLA \cdot Den \quad \text{(Eq. 1)}$$

$$Rad_{int} = Rad \cdot \left(1 - e^{-0.8LAI}\right) \quad \text{(Eq. 2)}$$

$$C_i = CO_2 \cdot \left(1 - \frac{1}{m \cdot RH}\right) \quad \text{(Eq. 3)}$$

$$Phot_{can} = \min(A_c, A_j, \frac{V_{cmax}}{2}) \quad \text{(Eq. 4)}$$

$$A_c = V_c \cdot \left(\frac{V_c \cdot (C_i - \Gamma^*)}{C_i + K_c \cdot \left(1 + \frac{O}{K_o}\right)}\right) \quad \text{(Eq. 5)}$$

$$V_c = V_{cmax} \cdot \left(\frac{31 + \frac{69}{1+e^{(-0.009 \cdot (Rad_{int} - 500)}}}{100}\right) \quad \text{(Eq. 6)}$$

$$A_j = \frac{J \cdot (C_i - \Gamma^*)}{(4C_i + 8\Gamma^*)} \quad \text{(Eq. 7)}$$

$$J = \frac{\alpha \cdot Rad_{int} + J_{max} - \sqrt{(\alpha \cdot Rad_{int} + J_{max})^2 - 4\theta \cdot J_{max} \cdot \alpha \cdot Rad_{int}}}{2\theta} \quad \text{(Eq. 8)}$$

The Arrhenius function was applied to reflect the temperature dependence of FvCB model parameters (Eq. 9-13). Leaf temperature, the main variable of the original model, was assumed to be the same as ambient temperature.

$$V_{cmax} = V_{25} \cdot \left(\frac{1+e^{\frac{(273.15+25) \cdot s - 202900}{25+273.15} \cdot R_{mol}}}{1+e^{\frac{(273.15+Temp_S) \cdot s - 202900}{R_{mol} \cdot (Temp_S+273.15)}}}\right) \cdot e^{\frac{91185 \cdot (Temp_S - 25)}{(25+273.15) \cdot R_{mol} \cdot (Temp_S+273.15)}} \quad \text{(Eq. 9)}$$

$$J_{max} = J_{25} \cdot \left(\frac{1+e^{\frac{(273.15+25) \cdot s - 201000}{25+273.15} \cdot R_{mol}}}{1+e^{\frac{(273.15+Temp_S) \cdot s - 201000}{R_{mol} \cdot (Temp_S+273.15)}}}\right) \cdot e^{\frac{79500 \cdot (Temp_S - 25)}{(25+273.15) \cdot R_{mol} \cdot (Temp_S+273.15)}} \quad \text{(Eq. 10)}$$

$$K_c = 404.9e^{\frac{79430 \cdot (Temp_S - 25)}{(25+273.15) \cdot R_{mol} \cdot (Temp_S+273.15)}} \quad \text{(Eq. 11)}$$

$$K_o = 278.4e^{\frac{36380 \cdot (Temp_S - 25)}{(25+273.15) \cdot R_{mol} \cdot (Temp_S+273.15)}} \quad \text{(Eq. 12)}$$

$$\Gamma^{*} = 42.75 e^{\frac{37830 \cdot (Temp_S - 25)}{(25+273.15) \cdot R_{mol} \cdot (Temp_S + 273.15)}} \quad \text{(Eq. 13)}$$

As environmental data were collected every 10 min as the second unit, the unit of $Phot_{can}$ (μmol $CO_2$ $m^{-2}$ $s^{-1}$) was converted to the amount of photo-assimilates per day, $A_{can}$ (g $CH_2O$ $plant^{-1}$ $d^{-1}$) as follows:

$$A_{can} = \sum_{1}^{86400} Phot_{can} \cdot 600 \text{ s} \cdot \frac{1 \text{mol}}{10^{6} \mu\text{mol}} \cdot \frac{30 \text{ g } CH_2O \text{ mol}^{-1}}{44 \text{ g } CO_2 \text{ mol}^{-1}} \cdot \frac{30 \text{ g } CH_2O}{\text{mol}} \cdot \frac{1}{Den} \quad \text{(Eq. 14)}$$

To estimate SSR (Eq. 15), source strength (Sour) (Eq. 16) and sink strength ($Sink_{tot}$) (Eq. 17) were calculated as follows (Wubs et al., 2012a; Zepeda et al., 2022):

$$SSR = \frac{\mathbf{Sour}}{\mathbf{Sink_{tot}}} \quad \text{(Eq. 15)}$$

$$\frac{d(Sour)}{dt} = \frac{d(A_{can})}{dt} - \frac{d(Resp_{main})}{dt} \cdot \left(1 - e^{-\frac{RGR}{3}}\right) + \frac{d(NSC)}{dt} \quad \text{(Eq. 16)}$$

$$Sink_{tot} = Sink_{veg} + Sink_{rep} \quad \text{(Eq. 17)}$$

$$Resp_{main} = (0.025 \cdot DM_{leaf}(t-1) + 0.025 \cdot DM_{stem}(t-1) + 0.01 \cdot DM_{root}(t-1) + 0.025 \cdot DM_{fruit}(t-1)) \cdot 2^{\frac{Temp_d - 25}{10}} \quad \text{(Eq. 18)}$$

Dark maintenance respiration ($Resp_{main}$) was reduced according to the average relative growth rate (RGR) of plants in the five preceding days (Eq. 16 and 18) (Heuvelink, 1995). This was adjusted because the maintenance respiration rate often

exceeds the assimilation rate when the radiation level is low, but the temperature is relatively high in greenhouses.

Vegetative sink strength ($Sink_{veg}$) (Eq. 19) and total reproductive sink strength ($Sink_{rep}$) were calculated based on $Temp_d$ and growing degree days (GDD) as follows (Eq. 20-24):

$$Sink_{veg} = C_{veg} \cdot Temp_d + Veg_{20} \quad \text{(Eq. 19)}$$

$$Sink_{fruit}(i) = \frac{\mathbf{1.35\ g\ CH_2O}}{\mathbf{g\ DM}} \cdot \frac{\mathbf{2\ stem}}{\mathbf{plant}} \cdot \frac{\mathbf{d(PDM_i)}}{\mathbf{dGDD_i}} \quad \text{(Eq. 20)}$$

$$PDM(i) = PFW(i) \cdot FDMC \quad \text{(Eq. 21)}$$

$$FDMC = \sin^2(0.3383 - 0.00084 \cdot (GDD_i - 78.778) \cdot e^{-0.00377 \cdot (GDD_i - 78.778)}) \quad \text{(Eq. 22)}$$

$$PFW(i) = \frac{\mathbf{W_{max}}}{\left(\mathbf{1+0.0305e^{-0.0619 \cdot (GDD_i - GDD_{init})}}\right)^{\frac{1}{0.0305}}} \quad \text{(Eq. 23)}$$

$$Sink_{rep} = \sum_{\mathbf{i=1}}^{\mathbf{N_t}} Sink_{\mathbf{fruit}}(\mathbf{i}) \quad \text{(Eq. 24)}$$

$$GDD = \sum_{\mathbf{i=1}}^{\mathbf{d}} \mathbf{Temp_d - T_{base}} \quad \text{(Eq. 25)}$$

GDD was calculated based on $Temp_d$ subtracted by the base temperature ($T_{base}$) of 10°C (Marcelis et al., 2006) (Eq. 25). Anthesis began when GDD exceeded $GDD_{init}$. Flowers appeared according to the flower appearance rate (FAR) per stem, which is dependent on GDD. The sink strength of individual fruit i ($Sink_{fruit}(i)$) was calculated with $GDD_i$ for every flower. It was multiplied by 2 to reflect two stems per plant (Eq. 20). When the moving average of SSR is below the threshold ($SSR_{thr}$) value, and it

was assumed that flowers do not generate due to abortion. Its moving average was calculated based on a two-day moving average of source strength and a five-day moving average of sink strength. Appeared flowers were assumed to not abort and set fruits two weeks after anthesis (Marcelis et al., 2004). The fruit was assumed to be harvested when it reached 2 g less than its maximum potential weight ($W_{max}$) or did not grow anymore.

Source strength determines the amount of photo-assimilates available for dry matter accumulation. The allocation to vegetative parts (root, stem, and leaf) (Eq. 26) and reproductive parts (flower and fruit) (Eq. 27) of a plant was determined based on the sink strength of each organ, which was calculated as follows:

$$DM_{veg} = Sour \cdot \frac{\mathbf{Sink_{veg}}}{\mathbf{Sink_{rep}+Sink_{veg}}} \cdot \frac{\mathbf{g\ DM}}{\mathbf{1.295\ g\ CH_2O}} \cdot \left(\mathbf{1} - \frac{\mathbf{1-\beta}}{\boldsymbol{\beta}}\right) \quad \text{(Eq. 26)}$$

$$DM_{rep} = Sour \cdot \frac{\mathbf{Sink_{rep}}}{\mathbf{Sink_{rep}+Sink_{veg}}} \cdot \frac{\mathbf{g\ DM}}{\mathbf{1.35\ g\ CH_2O}} \cdot \left(\mathbf{1} - \frac{\mathbf{1-\beta}}{\boldsymbol{\beta}}\right) \quad \text{(Eq. 27)}$$

$$DM_{org}(t) = \sum_{\mathbf{1}}^{\mathbf{t}} \mathbf{C_{org\_veg}} \cdot \mathbf{DM_{veg}} \quad \text{(Eq. 28)}$$

$$DM_{fruit}(t) = \sum_{\mathbf{i=1}}^{\mathbf{N_t}} \frac{\mathbf{Sink_{fruit}(i)}}{\mathbf{Sink_{rep}}} \cdot \mathbf{DM_{rep}} \quad \text{(Eq. 29)}$$

$\left(1 - \frac{1-\beta}{\beta}\right)$ was multiplied because the photo-assimilates are primarily used for growth respiration (Eq. 26 and 27). The rest of the photo-assimilates were partitioned to vegetative organs $DM_{org}(t)$ ($DM_{stem}(t)$, $DM_{stem}(t)$, and $DM_{stem}(t)$) and individual fruits based on the partitioning coefficient $C_{org\_veg}$ ($C_{leaf}$, $C_{stem}$, and $C_{root}$) and

individual fruit sink strength ($Sink_{fruit}$), respectively (Eq. 28 and 29). Therefore, total dry matter (TDM) was calculated as follows:

$$\mathrm{TDM(t)} = \sum_{z=1}^{t}\left(\mathbf{DM_{leaf}(z)} + \mathbf{DM_{stem}(z)} + \mathbf{DM_{root}(z)} + \mathbf{DM_{fruit}(z)}\right) \quad \text{(Eq. 30)}$$

It was assumed there is a carbon pool where carbon dioxide is imported through photosynthesis and converted into carbohydrates. When there were remaining carbohydrates after the allocation to plant organs, which were regarded as non-structural carbohydrates (NSC), these were added to the source strength of the next day. Thus, the NSC concentration was calculated as follows:

$$\frac{\mathbf{d(NSC)}}{\mathbf{dt}} = \frac{\mathbf{d(A_{can})}}{\mathbf{dt}} - \frac{\mathbf{d(Resp_{main})}}{\mathbf{dt}} - \mathbf{TDM(t)} \quad \text{(Eq. 31)}$$

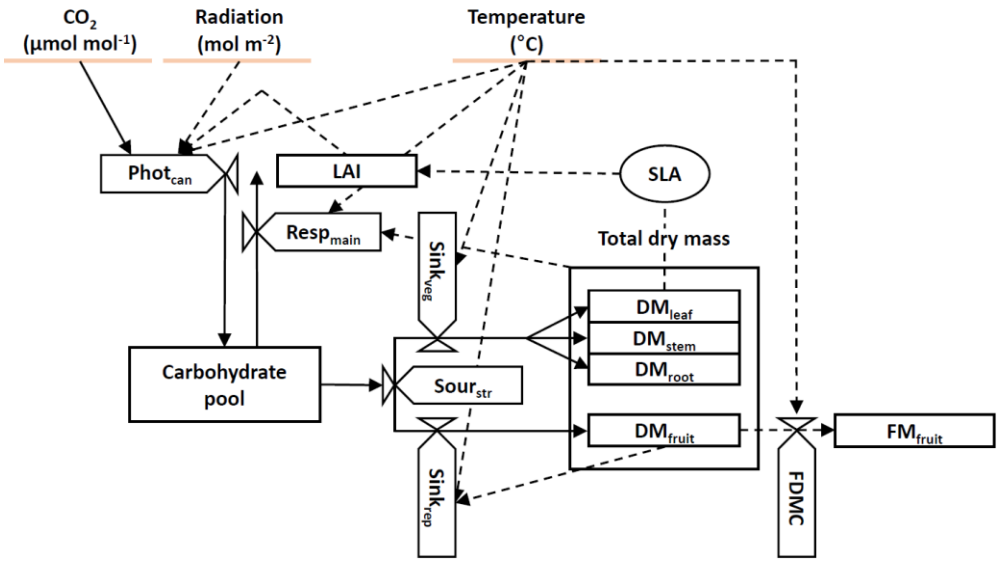


Fig. 2. A schematic diagram of the crop growth model INTKAM. Dashed arrows and line arrows represent information flow and mass flow, respectively. Red bars, rectangles, valve figures, and circles represent input variables, state variables, rate variables, and parameters, respectively. All the definitions of abbreviated variables are summarized in Table 3.

Table 2. List of parameters used in the INTKAM model.

| Parameter | Value | Unit | Definition |
|---|---|---|---|
| $C_{leaf}$ | 0.495 | - | Coefficient of photo-assimilate partitioning to leaves |
| $C_{root}$ | 0.1 | - | Coefficient of photo-assimilate partitioning to roots |
| $C_{stem}$ | 0.405 | - | Coefficient of photo-assimilate partitioning to stems |
| $CO_2$ | 400 | μmol mol $^{-1}$ | Ambient $CO_2$ concentration |
| $J_{25}$ | 150.8 | μmol $CO_2$ $m^{-2}$ $s^{-1}$ | Maximum electron transport rate at 25°C |
| m | 6.698 | - | Empirical parameter |
| O | 210 | μmol $mol^{-1}$ | Oxygen concentration |
| $R_{mol}$ | 8.314 | J $K^{-1}$ $mol^{-1}$ | Molar gas constant |
| s | 650 | J $K^{-1}$ $mol^{-1}$ | Entropy factor |
| $T_{base}$ | 10 | °C | Base temperature |
| $V_{25}$ | 83.4 | μmol $CO_2$ $m^{-2}$ $s^{-1}$ | Maximum carboxylation capacity at 25°C |
| $Veg_{20}$ | 1.6 | g $CH_2O$ plant$^{-1}$ $d^{-1}$ | Vegetative sink strength at 20°C |
| $W_{max}$ | 225 | g | Maximum fresh weight of a single fruit |
| α | 0.42 | mol $mol^{-1}$ | Light energy conversion efficiency on incident light |
| β | 0.8 | - | Yield factor for growth respiration |
| θ | 0.25 | - | The curvature of the light response of J |

Table 3. List of variables used in the INTKAM model. Brackets were used to indicate individual fruit or time.

| Variable | Unit | Definition |
|---|---|---|
| $A_c$ | μmol $CO_2$ $m^{-2}$ $s^{-1}$ | Net assimilation rate limited by Rubisco activity |
| $A_{can}$ | g $CH_2O$ $plant^{-1}$ $d^{-1}$ | Amount of photo-assimilate in plant canopy |
| $A_j$ | μmol $CO_2$ $m^{-2}$ $s^{-1}$ | Net assimilation rate limited by RuBP regeneration |
| $C_i$ | μmol $mol^{-1}$ | Intercellular $CO_2$ concentration |
| $DM_{rep}$ | g DM $plant^{-1}$ $d^{-1}$ | Dry matter allocated to reproductive organs |
| $DM_{fruit}(t)$ | g DM $plant^{-1}$ $d^{-1}$ | Dry matter of fruits at day t |
| $DM_{leaf}(t)$ | g DM $plant^{-1}$ $d^{-1}$ | Dry matter of leaves at day t |
| $DM_{root}(t)$ | g DM $plant^{-1}$ $d^{-1}$ | Dry matter of roots at day t |
| $DM_{stem}(t)$ | g DM $plant^{-1}$ $d^{-1}$ | Dry matter of stems at day t |
| $DM_{veg}$ | g DM $plant^{-1}$ $d^{-1}$ | Dry matter allocated to vegetative organs |
| FDMC | - | Fruit dry matter contents |
| GDD | °C d | Growing degree days |
| $GDD_i$ | °C d | Growing degree days of fruit i |
| J | μmol $CO_2$ $m^{-2}$ $s^{-1}$ | Electron transport rate |
| $J_{max}$ | μmol $CO_2$ $m^{-2}$ $s^{-1}$ | Maximum electron transport rate |
| $K_c$ | μmol $mol^{-1}$ | Michaelis-Menten constant of Rubisco for $CO_2$ |
| $K_o$ | μmol $mol^{-1}$ | Michaelis-Menten constant of Rubisco |
| LAI | $m^2$ $m^{-2}$ | Leaf area index |
| NSC | g $CH_2O$ $plant^{-1}$ $d^{-1}$ | Nonstructural carbohydrate |

| | | |
|---|---|---|
| $N_t$ | fruit | Number of fruits on day t |
| PDM(i) | g DM $fruit^{-1}$ $°C^{-1}$ $d^{-1}$ | Potential dry matter of fruit i |
| PFW(i) | g DM $fruit^{-1}$ $°C^{-1}$ $d^{-1}$ | Potential fresh weight of fruit i |
| $Phot_{can}$ | µmol $CO_2$ $m^{-2}$ $s^{-1}$ | Canopy photosynthesis |
| Rad | µmol $m^{-2}$ $s^{-1}$ | Photosynthetically active radiation (400 - 700 nm) |
| $Rad_{int}$ | µmol $m^{-2}$ $s^{-1}$ | Intercepted radiation to plants |
| $Resp_{gro}(t)$ | g $CH_2O$ $plant^{-1}$ $d^{-1}$ | Growth respiration at day t |
| $Resp_{main}(t)$ | g $CH_2O$ $plant^{-1}$ $d^{-1}$ | Maintenance dark respiration at day t |
| RGR | g DM $plant^{-1}$ $d^{-1}$ | 5d moving average of relative growth rate |
| RH | % | Relative humidity |
| $Sink_{fruit}(i)$ | g $CH_2O$ $fruit^{-1}$ $°C^{-1}$ $d^{-1}$ | Sink strength of an individual fruit i |
| $Sink_{rep}$ | g $CH_2O$ $plant^{-1}$ $d^{-1}$ | Reproductive sink strength of all fruits |
| $Sink_{tot}$ | g $CH_2O$ $plant^{-1}$ $d^{-1}$ | Total sink strength |
| $Sink_{veg}$ | g $CH_2O$ $plant^{-1}$ $d^{-1}$ | Vegetative sink strength |
| Sour | g $CH_2O$ $plant^{-1}$ $d^{-1}$ | Source strength |
| SSR | - | Source-sink ratio |
| t | d | Day |
| TDM(t) | g DM $plant^{-1}$ $d^{-1}$ | Total dry matter of a plant on day t |
| $Temp_d$ | °C | Mean ambient temperature per day |
| $Temp_s$ | °C | Ambient temperature per second |
| $V_c$ | µmol $CO_2$ $m^{-2}$ $s^{-1}$ | Carboxylation capacity at a specific light intensity |
| $V_{cmax}$ | µmol $CO_2$ $m^{-2}$ $s^{-1}$ | Maximum carboxylation capacity |
| $\Gamma^*$ | µmol $mol^{-1}$ | $CO_2$ compensation point |

**Model calibration**

The model was calibrated with leaf area, fruit dry weight, and total dry weight of vegetative organs measured during the 2020W period. Due to the relative deficiency of fruit dry weight data compared to fruit fresh weight data, some fruit dry weight data were linearly regressed from fruit fresh weight data. As ripened fruits were harvested and measured regardless of weight, fruits lighter than the first quantile (122 g) of harvested fruits were excluded from the calibration data. This was also applied when estimating fruit yield in the INTKAM simulation.

Parameters affected by radiation and temperature but lack explanatory models to express them were calibrated using the Bayesian optimization method and later fine-tuned manually (Lee and Heuvelink, 2003; Marcelis et al., 1998; Wubs et al., 2009). HyperOpt was used as a calibration algorithm to optimize sets of parameters while simultaneously maximizing or minimizing the objective function (Bergstra et al., 2015; Moon et al., 2023). Each parameter range was determined based on the data from destructive harvests or literature (Table 1). Normalized root mean squared error (NRMSE) was used to evaluate the objective function. Calibrated parameters were used for the model simulation.

Table 4. Parameters optimized using HyperOpt.

| Parameter | Unit | Description | Range | Distribution |
|---|---|---|---|---|
| $C_{veg}$ | g $CH_2O$ $°C^{-1}$ $plant^{-1}$ | Vegetative sink strength rate | [0.05, 0.2] | uniform |
| SLA | $m^2$ $g^{-1}$ | Specific leaf area | [0.15, 0.04] | uniform |
| $GDD_{init}$ | °C d | Growing degree days until the first anthesis | [400, 420] | uniform |
| FAR | flower $°C^{-1}$ $d^{-1}$ $stem^{-1}$ | Flower appearance rate per stem | [0.025, 0.045] | uniform |
| $SSR_{thr}$ | - | Source-sink ratio threshold | [1.0, 1.06] | uniform |

**Definition of PTR**

In this experiment, two different types of PTR were defined. The definition from the literature (Liu and Heins, 1997) and PTR that takes fruit load into account were compared as follows:

$$\mathrm{PTR} = \frac{\mathbf{DLI}}{\mathbf{Temp_d - T_{base}}} \quad \text{(Eq. 32)}$$

$$\mathrm{PTR_{fruit}} = \frac{\mathbf{DLI}}{\mathbf{Temp_d - T_{base} + 2 \cdot fruit\ load}} \quad \text{(Eq. 33)}$$

where DLI is daily light integral (mol $m^{-2}$ $day^{-1}$). $T_{base}$ was subtracted to reflect the thermal effect of temperature.

The average PTR for the 60 d prior to the final harvest was defined as the average PTR during the fruit developing stage. As fruits were set irregularly, the last fruit harvest was defined whenever the load became zero. The period between the beginning of anthesis and the last fruit harvest was considered a harvesting cycle. That is, as yield fluctuates, multiple harvesting cycle occurs.

**Simulation study with artificial data**

The random walk was applied to generate 100 radiation and temperature conditions (Ahn et al., 2022) (Fig. 3). It was assumed that clouds randomly cover the sky, thereby stochastically generating various light conditions. An empirical

coefficient derived from weather station data was applied to reflect the radiation dependence of temperature as follows:

$$Ta' = Rad' \cdot a + b \quad \text{(Eq. 34)}$$

where Ta´ is artificial temperature (°C), and Rad´ is artificial radiation (μmol $m^{-2}$ $s^{-1}$). a and b change randomly between 16 to 44 and 14.85 to 16.85, respectively. In the simulation, planting density was assumed to be 3 plant $m^{-2}$, and the cultivation period was set to one year.

In this experiment, INTKAM was again modified, called $INTKAM_{con}$. Both models were simulated under the same conditions to examine the effect of SSR on the relationship between PTR and yield in indeterminate fruit crops. In $INTKAM_{con}$, it was assumed that flowers appear at a constant rate of 0.007 flower $°C^{-1}$ $d^{-1}$ $stem^{-1}$ so that FAR is not affected by $SSR_{thr}$. This was calculated by multiplying the reported value of flower appearance rate per stem with its survival rate (= 1 − abortion rate) at a planting density of 3.1 plant $m^{-2}$, which were 0.035 flower $°C^{-1}$ $d^{-1}$ $stem^{-1}$ and 0.2, respectively (Marcelis et al., 2004; Elings and de Visser, 2011).

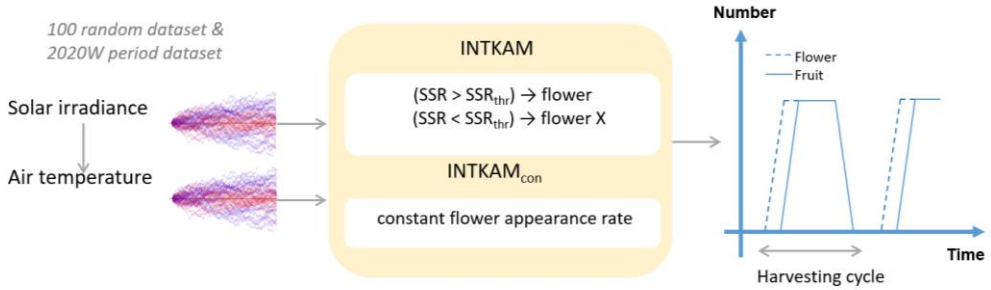


Fig. 3. A schematic diagram of the model simulation. The model was simulated with 100 artificial data of radiation and temperature, as well as the environmental dataset of the 2020W period. In artificial data, it was assumed that solar radiation affected air temperature. In INTKAM, flowers appeared when the source-sink ratio (SSR) was above the threshold ($SSR_{thr}$), while in $INTKAM_{con}$, the flower appearance rate was set as a constant value. The dashed blue line indicates the number of flowers that appeared, and the solid blue line indicates the number of fruits that were set and harvested throughout the harvesting cycle.

# RESULTS

## Calibration result

INTKAM parameters, SLA, $SSR_{thr}$, $GDD_{init}$, FAR, and $C_{veg}$ were calibrated as 0.02 $m^2\ g^{-1}$, 1.03, 410°C d, 0.034 flower $°C^{-1}\ d^{-1}\ stem^{-1}$, and 0.09 g $CH_2O\ °C^{-1}\ plant^{-1}$, respectively (Fig. 4). While SLA and $C_{veg}$ were lower than the reported values from the growth analysis of sweet peppers (Nilwik, 1981; Wubs, 2012b), other values were similar to the reported values for large-fruited cultivars (Wubs et al., 2009; Elings and Visser., 2011).

Root mean squared error (RMSE) for total dry weight of vegetative organs (a), leaf area (b), and cumulative fruit dry weight (c) were 25.77 g $plant^{-1}$, 0.19 $m^2\ plant^{-1}$, and 77.61 g $plant^{-1}$, respectively. The cumulative fruit fresh weight (d) was estimated using (Eq. 21). The model overestimated vegetative growth when fruits were started to be harvested. Its RMSE was 0.005 kg $plant^{-1}$.

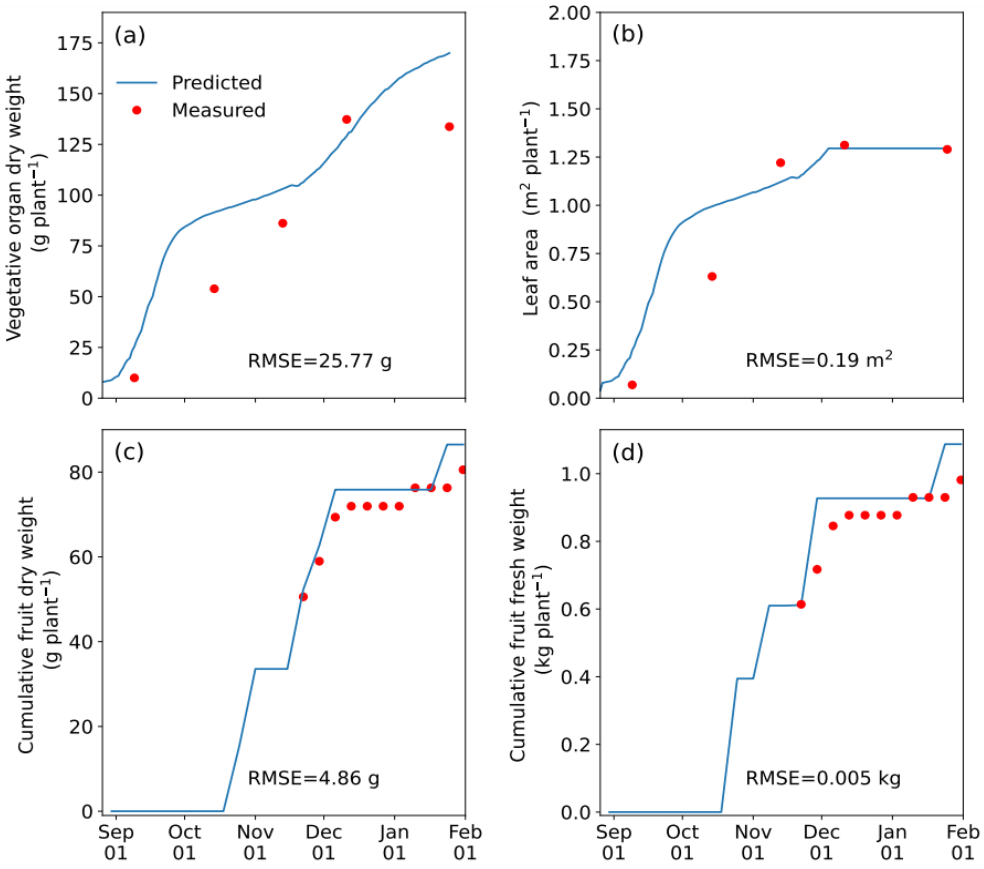


Fig. 4. Calibration result of INTKAM for the 2020W period. The model was fitted to the total dry weight of vegetative organs (a), leaf area (b), and cumulative fruit dry weight (c). The cumulative fruit fresh weight (d) was estimated based on the calibrated parameters. Red points indicate measured values, and the blue lines indicate the prediction of the model.

**Relationship between PTR and fruit yield**

First, when the relationship between the fruit yield and the average photothermal ratio (PTR) for the 60 d prior to the final harvest was investigated from the dataset of three cultivation periods, the squared correlation coefficient was 0.14, indicating weak linearity (Fig. 5a). A similar tendency was observed from the simulation result of INTKAM with various radiation and temperature conditions. The squared correlation coefficient between the PTR and the simulated fruit yield was 0.1. These results indicated no strong linearity between the PTR and fruit yield.

When $INTKAM_{con}$ was simulated with the same conditions, the correlation coefficient between the PTR and the simulated fruit yield was 0.61, which indicates strong linearity (Fig. 5b).

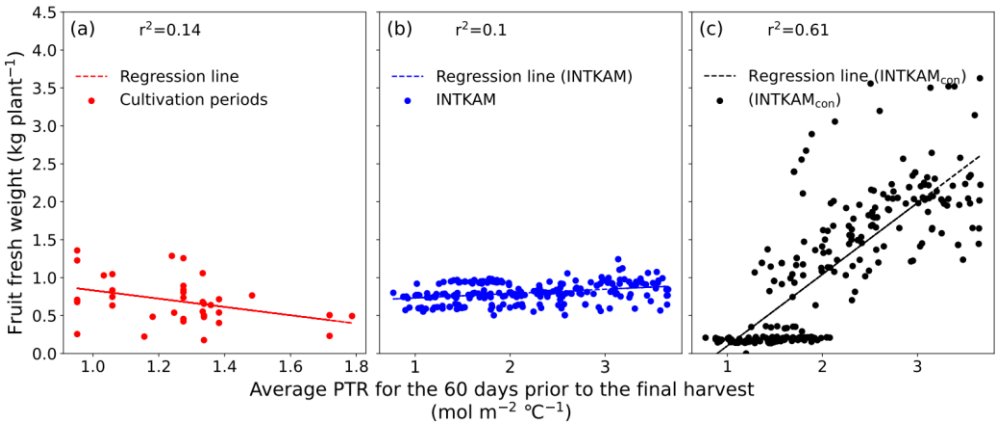


Fig. 5. The relationship between the fruit yield and the average photothermal ratio (PTR) for the 60 d prior to the final harvest. The dataset from the three cultivation periods (red) (a), the INTKAM simulation (blue) (b), and the $INTKAM_{con}$ simulation (black) (c) were analyzed. $r^2$ is a squared correlation coefficient, indicating the intensity of linearity. Dashed lines are regression lines of each dataset. $INTKAM_{con}$ is a modified INTKAM that assumes a constant flower appearance rate.

**Comparison between the change of SSR and PTR**

The SSR change was compared with the PTR and the $PTR_{fruit}$ that was modified to take fruit load into account (Fig. 6). The coefficient of determination ($R^2$) was used to evaluate the consistency between the explanatory variable and dependent variable. As a result, $R^2$ between PTR and SSR was −1.32 while the $R^2$ between $PTR_{fruit}$ and SSR was 0.55. In other words, $PTR_{fruit}$ was more similar to the pattern of SSR change than PTR.

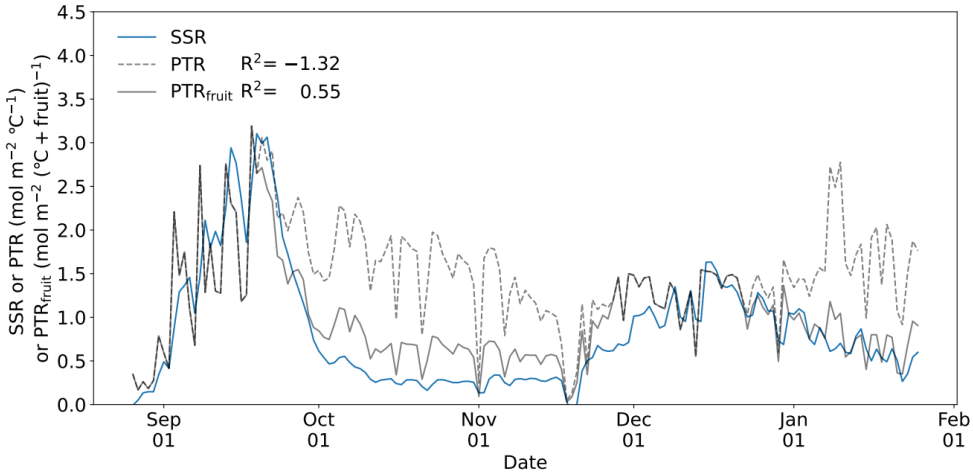


Fig. 6. The change of source-sink ratio (SSR) (blue line), photothermal ratio (PTR) (grey dashed line), and PTR that reflects fruit load ($PTR_{fruit}$) (grey solid line) according to days in the 2020W period. $R^2$ value represents the coefficient of determination, which shows how well the PTR and $PTR_{fruit}$ can explain the SSR.

**Relationship between the $PTR_{fruit}$ and fruit yield**

While the fruit yield was similar regardless of average PTR (Fig. 7a), the high fruit yield (higher than 0.9 kg $plant^{-1}$) was in the $PTR_{fruit}$ range of 0.5-2.0 mol $m^{-2}$ (fruit + °C)$^{-1}$ (Fig. 7b). The fruit yield lower than 0.9 kg $plant^{-1}$ was also formed in wider $PTR_{fruit}$ range. In other words, when the average $PTR_{fruit}$ for the 60 d prior to the final harvest deviates from the specific range, this can result in lower fruit yield.

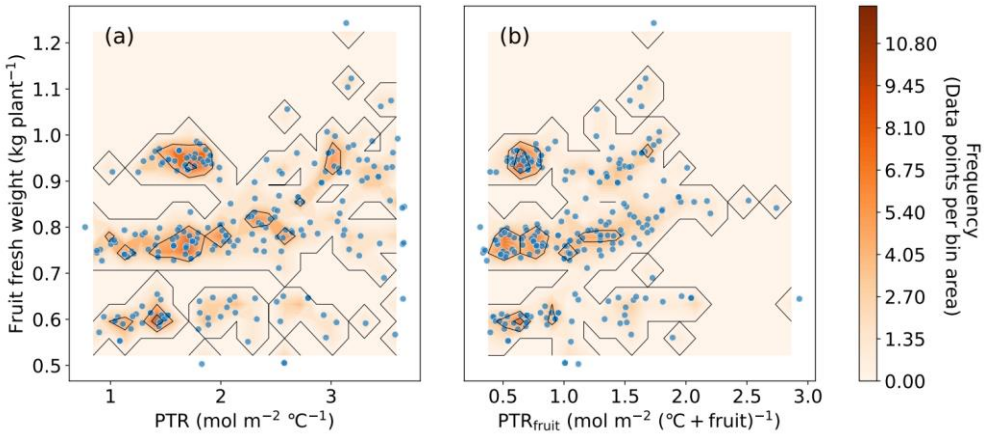


Fig. 7. Comparison of the relationship between PTR and the fruit fresh weight (a), and the relationship between $PTR_{fruit}$ and the fruit fresh weight (b). The color bar indicates the number of data points per bin area.

# DISCUSSION

Calibrating parameters is important for the model simulation as it can significantly influence the interpretation of the real world. Although numerous combinations of parameters were tested through HyperOpt and manual adjustment, it was impossible to find the parameters that could accurately explain vegetative and reproductive growth simultaneously. One of the main reasons for this was $GDD_{init}$, which determines the timing of the first anthesis. When $GDD_{init}$ was changed to 300°C d, while other parameters were the same, the RMSE was 16.46 g and 0.14 $m^{-2}$ for the total dry weight of vegetative organs and leaf area, which were lower than the corresponding RMSE in this study (Fig. 4). However, this resulted in an 11.23 g RMSE in fruit dry weight estimation, which is higher than the corresponding value in this study. It was because the model estimated the occurrence of the second harvesting cycle at the end of the cultivation period, which was not true. As the research aims to investigate the relationship between fruit yield and PTR, the parameters were fine-tuned to represent the fruit-setting pattern accurately.

The relationship between the fruit yield of sweet peppers and the average PTR during the fruit developing stage (Fig. 5a and 5b) contradicts the results of other studies that reported a linear relationship (Poggio et al., 2005). This was contributable to fruit-setting pattern of sweet peppers. Fruits were set irregularly because flowers appeared and aborted depending on the threshold ($SSR_{thr}$) value. In the INTKAM simulation, only when SSR is higher than the $SSR_{thr}$, flowers appear (Fig. 3 and S1),

which is the common trait of indeterminate fruit crops (Heuvelink et al., 2004). When the effect of the SSR on the fruit-setting pattern was removed in $INTKAM_{con}$, flower appearance and fruit development were solely dependent on temperature and radiation, as FAR is based on GDD (Table 4), and the assimilation rate is driven by radiation level.

A higher PTR indicates a relatively higher radiation level or lower temperature. This condition induces more photo-assimilate assimilation, less respiration consumption, and slower fruit development. Consequently, it allows more carbohydrates to be accumulated in fruits, leading to a higher yield. This explains the linear relationship between the yield simulated from $INTKAM_{con}$ and the average PTR during fruit development (Fig. 5c).

While radiation is the main driver of source strength, temperature is the main driver of respiration, vegetative sink strength, and reproductive sink strength. Thus, PTR can provide insight into the balance between assimilation and consumption of photo-assimilates (Poorter et al., 2016). However, the current definition of PTR only contains environmental variables in its definition (Eq. 32) (Liu and Heins, 1997). This is insufficient to reflect the balance state of photo-assimilates, which is expressed as SSR (Eq. 15) (Fig. 6). This is mainly due to reproductive sink strength ($Sink_{rep}$), which is driven by GDD. Thus, DMT in PTR cannot represent the total sink strength of a plant. This can limit the utility of PTR as an indicator for greenhouse climate management (Geelen et al., 2021).

This study considered fruit load in the $PTR_{fruit}$ calculation because the change in fruit load has a similar pattern to $Sink_{rep}$ (Fig. S1), which was also confirmed by Elings and de Visser (2011). As a result, while existing PTR showed a similar tendency but a different value with SSR, $PTR_{fruit}$ showed higher consistency with SSR values (Fig. 6). In other words, DLI, DMT, and plant load could represent source strength, vegetative sink strength, and reproductive sink strength, respectively, in $PTR_{fruit}$.

Furthermore, the scatterplot between fruit yield and $PTR_{fruit}$ (Fig. 7) revealed that fruits were harvested within the specific range of $PTR_{fruit}$. This was more evident when the relationship between the average SSR for the 60d prior to the final harvest and the fruit fresh weight was analyzed (Fig. S2). That is, plants might not perform the best when either the source or sink strength is relatively too strong. Thus, these results demonstrate that $PTR_{fruit}$ should be maintained within a specific range to avoid low fruit yield. Besides, given that fruit load is easy to measure, $PTR_{fruit}$ can be a better indicator for monitoring the current photo-assimilate balance state of plants and regulating the greenhouse environment.

**Limitations of the current study and further approach**

This study simplified the pattern of flower appearance and fruit set by regulating them based on the SSR threshold (Fig. 6). However, sweet pepper flowers have a critical time before and after the anthesis where they are vulnerable to environmental and growth conditions (Marcelis et al., 2004; Wubs et al., 2011). During this time, numerous flowers appear continuously, and some of them are aborted when the

average SSR is below the threshold. Thus, the assumption that flowers do not appear below the threshold value could lead to an underestimation of reproductive sink strength and an inaccurate description of the dynamic change in the number of flowers and fruits (Fig. 6).

The current study randomly generated various radiation and temperature conditions using random walks without considering the effect of greenhouse climate management. However, better insight could have been derived if PTR was linked to an active climate control strategy, such as turning on artificial lighting only when the daily radiation level in subsequent days is expected to be lower than the threshold. Such an approach can be further extended to balance energy use and yield (Elings et al., 2006; Katzin et al., 2021). Through simulating an explanatory model in various radiation and temperature conditions, one can estimate the amount of energy required to attain the desired yield.

# CONCLUSION

In this study, the relationship between PTR and the yield of indeterminate fruit crops was examined. Strong linearity was not observed when this relationship was analyzed with the harvest data of cultivation periods. A simulation study with an explanatory crop model, INTKAM, corroborated this. However, strong linearity was observed when simulated in the same condition with a constant flower appearance rate, indicating that non-linearity was ascribable to the SSR that regulates fruit setting patterns.

The study further delved into the relationship between SSR, PTR, and fruit yield. As a result, PTR showed a higher similarity with SSR change when the fruit load was taken into account in the calculation. This was because fruit load according to time had a similar pattern with $Sink_{rep}$. This was reflected in the modified PTR ($PTR_{fruit}$) calculation, showing higher consistency with the SSR change. Furthermore, its relationship with fruit yield revealed the importance of maintaining it within a limited range. In conclusion, $PTR_{fruit}$ is more useful in greenhouse climate management than PTR when it comes to balanced crop growth because it reflects the plant assimilation and consumption state of photo-assimilates more accurately.

# LITERATURE CITED


Ahn TI, Jung JH, Kim HS, Lee JY (2022) Translating $CO_2$ variability in a plant growth system into plant dynamics. Sci Rep 1–10

Bergstra J, Komer B, Eliasmith C, Yamins D, Cox DD (2015) Hyperopt: A Python library for model selection and hyperparameter optimization. Comput Sci Discov 8

Bertin N (2005) Analysis of the tomato fruit growth response to temperature and plant fruit load in relation to cell division, cell expansion and DNA endoreduplication. Ann Bot 95:439–447

Elings A, De Zwart HF, Janse J, Marcelis LFM, Buwalda F (2006) Multiple-day temperature settings on the basis of the assimilate balance: A simulation study. Acta Hortic 718:219–226

Elings A, Meinen E, Campen J, Stanghellini C (2007) The Photosynthesis Response of Tomato to Air Circulation. Acta Hortic 761:77–84

Elings A, De Visser PHB (2011) Modelling Fruit Set in Greenhouse Vegetable Crops. Acta Hortic 761:757–764

Geelen PA, Voogt JO, van Weel PA (2021) Plant Empowerment: The Basic Principles (3rd edition). Plant Empowerment T Academy. The Netherlands: Letsgrow

Heuvelink E (1995) Dry Matter Production in a Tomato Crop : Measurements and Simulation. Ann Bot 75:369–379

Heuvelink E (1999) Evaluation of a Dynamic Simulation Model for Tomato Crop Growth and Development. Ann Bot 83:413–422

Heuvelink E, Marcelis LFM, Körner O (2004) How to reduce yield fluctuations in sweet pepper? Acta Hortic 633:349–355

Hirose T (2005) Development of the Monsi–Saeki theory on canopy structure and function. Ann Bot 95:483−494

Homma M, Watabe T, Ahn DH, Higashide T (2022) Dry Matter Production and Fruit Sink Strength Affect Fruit Set Ratio of Greenhouse Sweet Pepper. J Am Soc Hortic Sci 147:270−280

Johansson H, Jones HJ, Foreman J, Hemsted JR, Stewart K, Grima R, Halliday KJ (2014) *Arabidopsis* cell expansion is controlled by a photothermal switch. Nat Commun 5:4848

Katzin D, Marcelis LFM, van Mourik S (2021) Energy savings in greenhouses by transition from high-pressure sodium to LED lighting. Appl Energy 281:16019

Lee JH, Heuvelink E (2003) Simulation of leaf area development based on dry matter partitioning and specific leaf area for cut chrysanthemum. Ann Bot 91:319–327

Li T, Heuvelink E, Marcelis LFM (2015) Quantifying the source-sink balance and carbohydrate content in three tomato cultivars. Front Plant Sci 6:416

Liu B, Heins RD (1997) Is plant quality related to the ratio of radiant energy to thermal energy? Acta Hortic 435:171–182

Liu B, Heins RD (2002) Photothermal Ratio Affects Plant Quality in 'Freedom' Poinsettia. J Am Soc Hortic Sci 127:20−26

Marcelis LFM (1994) A simulation model for dry matter partitioning in cucumber. Ann Bot 74:43–52

Marcelis LFM, Heuvelink E, Baan Hofman-Eijer LR, Den Bakker J, Xue LB (2004) Flower and fruit abortion in sweet pepper in relation to source and sink strength. J Exp Bot 55:2261–2268

Marcelis LFM, Elings A, Dieleman JA, De Visser PHB, Bakker MJ, Heuvelink E (2006) Modelling dry matter production and partitioning in sweet pepper. Acta Hortic 718:121−128

Menéndez FJ, Satorre EH (2007) Evaluating wheat yield potential determination in the Argentine Pampas. Agric syst 95:1−10

Moccaldi LA, Runkle ES (2007) Modeling the effects of temperature and photosynthetic daily light integral on growth and flowering of *Salvia splendens* and *Tagetes patula*. J Am Soc Hortic Sci 32:283−288

Moon T, Sim S, Son JE (2023) Calibration of food and feed crop models for sweet peppers with Bayesian optimization. Hortic Environ Biotechnol 1−11

Moore CE, Meacham-Hensold K, Lemonnier P, Slattery RA, Benjamin C, Bernacchi CJ, Lawson T, Cavanagh AP (2021) The effect of increasing temperature on crop photosynthesis: from enzymes to ecosystems. J Exp Bot 72:2822-2844

Nilwik HJM (1981) Growth analysis of sweet pepper (*Capsicum annuum* L.) 1. The influence of irradiance and temperature under glasshouse conditions in winter. Ann Bot 48:129-136

Poggio SL, Satorre EH, Dethiou S, Gonzalo GM (2005) Pod and seed numbers as a function of photothermal quotient during the seed set period of field pea (*Pisum sativum*) crops. Eur J Agron 22:55-69

Poorter H, Fiorani F, Pieruschka R, Wojciechowski T, van der Putten WH, Kleyer M, Schuur U, Postma J (2016) Pampered inside, pestered outside? Differences and similarities between plants growing in controlled conditions and in the field. New Phytol 212:838–855

Sadras V, Dreccer MF (2015). Adaptation of wheat, barley, canola, field pea and chickpea to the thermal environments of Australia. Crop Pasture Sci 66:1137-1150

Sánchez-Molina JA, Pérez N, Rodríguez F, Guzmán JL, López JC (2015) Support system for decision making in the management of the greenhouse environmental based on growth model for sweet pepper. Agric Syst 139:144–152

Shin J, Hwang I, Kim D, Kim J, Hyun J, Son JE (2022) Waning advantages of $CO_2$ enrichment on photosynthesis and productivity due to accelerated phase transition and source-sink imbalance in sweet pepper. Sci Hortic 301:111130

Wubs AM, Bakker MJ, Heuvelink E, Hemerik L, Marcelis LFM (2006) Stochastic simulation of fruit set in sweet pepper. Proc. - Second Int. Symp. Plant Growth Model. Simulation, Vis. Appl. PMA 2006:40–47

Wubs AM, Ma YT, Heuvelink E, Marcelis LFM (2009) Genetic differences in fruit-set patterns are determined by differences in fruit sink strength and a source: sink threshold for fruit set. Ann Bot 104:957–964

Wubs AM, Heuvelink E, Marcelis LFM, Hemerik L (2011) Quantifying abortion rates of reproductive organs and effects of contributing factors using time-to-event analysis. Funct Plant Biol 38:431-440

Wubs AM, Ma YT, Heuvelink E, Hemerik L, Marcelis LFM (2012a) Model selection for nondestructive quantification of fruit growth in pepper. J Am Soc Hortic Sci 137:71–79

Wubs AM (2012b) Towards stochastic simulation of crop yield: a case study of fruit set in sweet pepper. Dissertation, Wageningen UR

Xu R, Dai J, Luo W, Yin X, Li Y, Tai X, Han L, Chen Y, Lin L, Li G, Zou C, Du W, Diao M (2010) A photothermal model of leaf area index for greenhouse crops. Agric For Meteorol 150:541–552

Zepeda AC, Heuvelink E, Marcelis LFM (2023) Carbon storage in plants: a buffer for temporal light and temperature fluctuations. in silico Plants 5:diac020

# ABSTRACT IN KOREAN

광과 온도는 식물의 광합성과 발달을 결정하는 핵심 요소이다. 따라서 최근 상업온실에선 일적산광량과 유효적산온도의 비율로 정의되는 광열비(photothermal ratio, PTR)를 활용하여 환경을 조절하고 있다. PTR 은 곡류의 수확량과는 선형적인 관계가 보고되어 있지만 source-sink 비율에 의해 착과 양상이 불규칙적으로 나타나는 무한생장형 과채류 작물에 대해선 이런 관계성이 적용되어 있지 않다. 이로 인해 PTR 을 온실 재배 지표로 활용하는 데 어려움이 있을 수 있다. 본 연구의 목적은 설명적 모델인 INTKAM 을 활용하여 PTR 과 착색 단고추의 광합성 및 분배과정과의 관계를 분석하고, 이를 바탕으로 수확량에 대해 더 설명력을 갖는 지표를 도출하는 것이다. 먼저 네 작기 동안 재배된 착색 단고추 (*Capsicum annuum* L. var. *annuum*)의 수확량 데이터와 과실 발달기간 동안의 평균 PTR 의 관계를 분석했다. 이 중 2020 년 겨울 작기를 기반으로 INTKAM 모델의 모수를 보정한 뒤 100 가지의 임의의 광-온도 조건에서 모델을 시뮬레이션 했다. 실제 수확량 분석 결과 평균 PTR 과 과일 수확량은 선형적인 관계가 관찰되지 않는 것으로 나타났으며 시뮬레이션 분석 결과 또한 동일한 양상이 나타났다. 그 원인은 식물의 현재 생육 상태를 나타내는 지표인 source-sink 비율이 임계점 (1.03) 이하일 때 새로 맺히는 꽃이 낙화되기 때문이며 이 영향을 없앤 뒤 시뮬레이션을 다시 돌려 선형성이 회복됨을 통해 이를 확인했다. 한편 PTR 계산시 현재 착과된 과실의 개수를

반영하면 한 작기 동안의 source-sink 비율과 높은 일치도를 보이는 것으로 나타났다. 또한, 보정된 PTR 이 0.5-2.0 mol $m^{-2}$ (fruit + °C)$^{-1}$ 범위 내로 과실 발달기동안 유지되었을 때 수확량이 상대적으로 높게 형성되는 것으로 나타났다. 해당 연구의 결과는 작물 모형을 통해 PTR 과 수확량의 관계를 생물학적 원리에 기반해 해석할 수 있음을 시사한다. 따라서 기존 PTR 보다는 보정된 PTR 이 온실 재배관리에 더욱 유용한 의사결정 지표이다.

추가 주요어: 설명적 모형, 무한생장형 과채류 작물, 광열비율, 소스 싱크 비율,
학 번: 2021-25491

# SUPPLEMENTARY INFORMATION

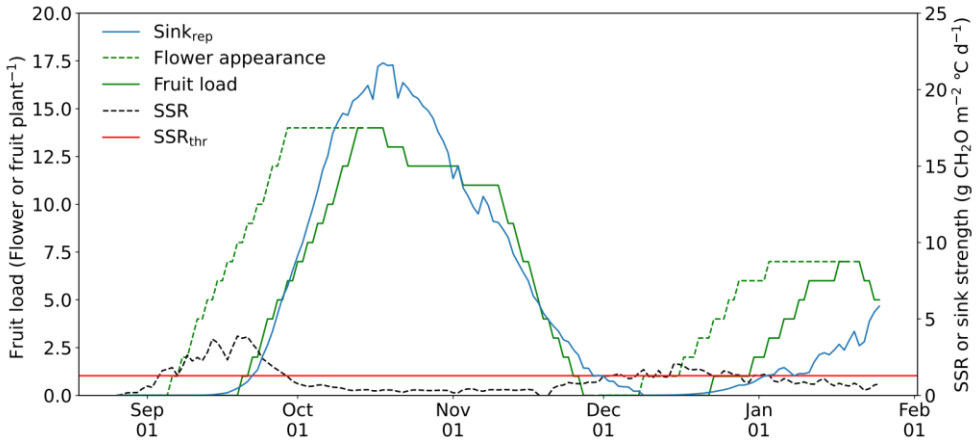


Fig. S1. Change of source-sink ratio (SSR) (black dashed line), number of flowers (green dashed line), number of fruits (green solid line), and reproductive sink strength ($Sink_{rep}$) (blue line) according to days in the 2020W period. All values were estimated through the INTKAM simulation. Flowers only appear when SSR is above the threshold ($SSR_{thr}$) value, illustrated as the red line. All the flowers appeared were assumed to be set after two weeks and harvested when they reached the maximum fruit weight.

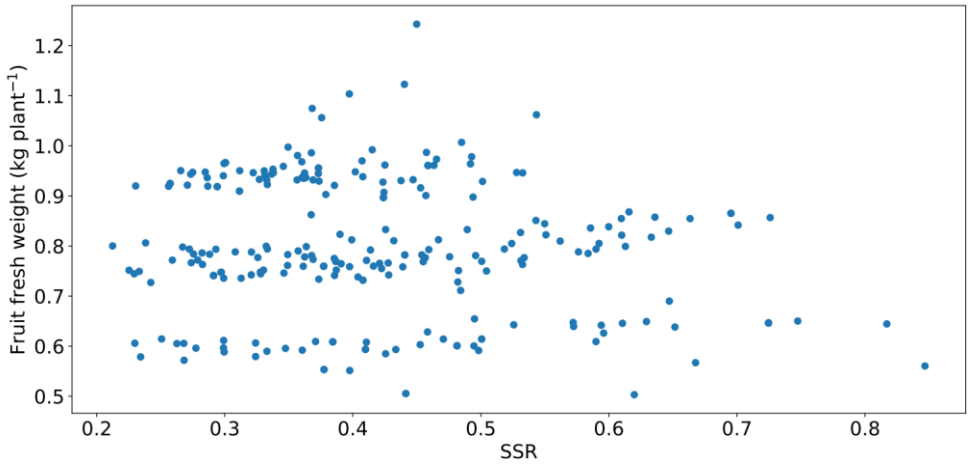


Fig. S2. The relationship between the average source-sink ratio (SSR) for the 60 d prior to the final harvest and the fruit fresh weight.